Hydration water, charge transport and protein dynamics.

Michel Peyrard
Laboratoire de Physique, Ecole Normale Supérieure de Lyon,
46 allée d'Italie, 69364 Lyon Cedex 07, France.

Abstract. The hydration water of proteins is essential to biological activity but its properties are not yet fully understood. A recent study of dielectric relaxation of hydrated proteins [A. Levstik et al., Phys. Rev E. **60** 7604 (1999)] has found a behavior typical of a proton glass, with a glass transition of about 268K. In order to analyze these results, we investigate the statistical mechanics and dynamics of a model of "two-dimensional water" which describes the hydrogen bonding scheme of bounded water molecules. We discuss the connection between the dynamics of bound water and charge transport on the protein surface as observed in the dielectric measurements.

1. Introduction

Water is well known to be essential for life. This is not only true at the level of organisms but also at the molecular level. Proteins are inactive in the dehydrated state. They begin their biological activity when their hydration level reaches approximately 0.2 g of water per g of protein, and attain a full activity with 1 g of water per g of protein [1, 2]. A direct observation of the effect of a small amount of hydration water on the dynamics of a protein has been provided by the experiment if Reinisch et al. [3] who used a high frequency quartz microbalance to probe the effects of water uptake on protein fluctuations.

Even before studying the effect of water on proteins, it is necessary to understand the properties of the hydration water itself. Those water molecules are hydrogen bonded to the protein which induces some drastic departure from the properties of bulk water. For instance a significant amount of water (0.3 – 0.4 g/g of protein) remains mobile down to temperatures so low that it has been called "unfreezable water" [1]. One experimental method of choice to study this bound water is provided by dielectric measurements because water molecules are highly polar and moreover they form a network on the surface of the protein along which protons can be transferred. The formation of this network with long range connectivity has been detected as a percolation transition when the water content approaches 0.5 g/g of protein [4]. More recently dielectric measurements [5] completed by a detailed analysis [6] have shown that, when temperature is reduced, the proton mobility slows down with an evolution characteristic of a proton

glass. In this paper, we analyze these results theoretically. Section 2 gives a brief summary of the results of the dielectric measurements and of the mechanism of proton transfer in hydration water. Section 3 introduces a model for hydration water and studies its thermodynamics and dynamics and section 4 discusses the results of the dielectric measurements in the light of the properties of bound water obtained in Sec. 3.

2. Dielectric properties of hydration water.

Early studies of hydrated lysozyme powders [4] in the frequency range 10 kHz to 10 MHz and studies of the isotope effect with D_2O-hydrated samples showed that protonic conduction is the dominating contribution to the dielectric relaxation in this frequency range. More recent experiments [5, 6] investigated the frequency and temperature dependence of the dielectric relaxation. The complex dielectric relaxation has been fitted by the Havrilak-Negami expression

$$\epsilon^\star = \epsilon_0 - (\epsilon_0 - \epsilon_\infty) \left[\frac{(i\omega\tau)^{1-\alpha}}{(1 + (i\omega\tau)^{1-\alpha})} \right]^{\beta} , \qquad (1)$$

where τ is a characteristic relaxation time, ϵ_0 is the static dielectric constant, ϵ_∞ the high frequency dielectric constant, and α and β parameters associated with the shape and width of the distribution of relaxation times.

The analysis of the dielectric measurements at various temperatures in the range 300–250 K shows that the relaxation time obeys a Vogel–Fulcher law

$$\frac{1}{\tau} = \nu = \nu_0 \exp\left[-\frac{E}{T - T_0} \right] \qquad (2)$$

generally associated to a glassy behavior. If one assumes that the dielectric relaxation results from a distribution of relaxation times, each obeying a Vogel–Fulcher law, by plotting for each measurement frequency the quantity

$$\frac{2}{\pi} \frac{\varepsilon''(\omega, T)}{\chi_0(T)(T - T_0)} \qquad \text{versus} \qquad (T - T_0) \ln(\nu_0/\nu)$$

one should obtain a plot which is the same for all frequencies [7]. Getting such a "master curve" is a sensitive indication of the existence of a glass transition in the system. The collapse on a single curve has been found for $Rb_{1-x}(NH_4)_xH_2PO_4$ which is a *proton glass* [7] and the same collapse is observed for the dielectric properties of weakly

hydrated protein above $T \approx 270$ K. Moreover a detailed analysis of the dielectric results versus temperature [6] shows that different part of the spectrum have a relaxation which diverges at slightly different freezing temperatures, all of them being however close to $T_0 \approx 268$ K. Below this temperature, the relaxation is found to obey a simple Arrhenius temperature dependence.

The measurements show that protonic conduction is at the origin of the dielectric relaxation, but, for water and ice, proton transport cannot be dissociated from the dynamics of the water itself. Already in 1980, Kunst et al. noticed that the temperature dependence of proton mobility in ice suggests a polaron mechanism *involving the motion of the oxygens* [8]. More recently, using methods of quantum chemistry, Lobaugh et al. [9] showed that proton transfer involves the $H_5O_2^+$ complex which provides a flat and broad potential on which an excess proton can move. The dynamics of excess protons in this potential is governed by solvent fluctuations, i.e. by the dynamics of the molecules around the complex. These results suggest that the slowing down of dielectric relaxation due to proton motion could well find its origin in a transition in the dynamics of the hydration water itself. An additional hint pointing in the same direction is provided by the calorimetric studies of Sartor et al. [1] which indicate a sharp change in the thermal motion of protein hydration water around 270 K.

3. Thermodynamics and dynamics of a model for surface water.

3.1. Model for hydration water.

The building block of a model for hydration water is indeed a description of the water molecule, but, in order to investigate the structure of the water patches on the surface of a weakly hydrated protein, we must also pay attention to the connectivity of these molecules. The remarkable property of water molecules is their ability to make hydrogen bonds in 4 directions that form a tetrahedra in space. Two of these directions are defined by the $O - H$ bonds, and the two others are associated to electronic orbitals of the oxygen. In ice, the water molecules are linked by hydrogen bonds along these 4 "arms". In liquid water some of the hydrogen bonds persist, at least as a temporary link between the molecules, and they are responsible of the anomalous properties of water, such as its density maximum around 4° C. Various models have been proposed to describe the potential energy of interacting water molecules. One of them, which is still rather simple but

gives good results when it is used for molecular dynamics simulations, is the "extended simple point charge potential" (SCP/E) which has been applied to the numerical simulation of supercooled water [10]. In such a model the interaction between two water molecules is described by a Lennard-Jones potential between the molecule centers and electrostatic interactions of effective charges associated to the protons and the oxygen. The water molecules which are attached to the surface of the protein do not have their 4 arms available for hydrogen bonding because one of them is used in the bond with the protein. Therefore the network of hydration-water molecules is built with molecules which have only three arms. This peculiarity allows us to describe hydration water with a model which is more convenient for computations than the SCP/E model, the Ben-Naim model [11, 12] which is schematically plotted in Fig. 1(a). The Ben-Naim model, which had been originally designed
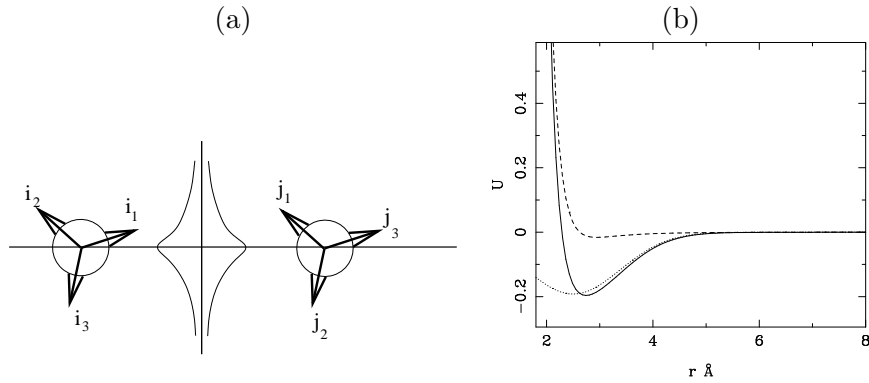
Figure 1. (a) Schematic picture of the Ben Naim interaction potential for two water molecules represented by disks with three arms. The curves between the two molecules show the Gaussian functions used to describe the orientational part of the hydrogen bond potential. (b) Interaction potential between two water molecules with two aligned arms as a function of their distances. The dash line shows the Lennard-Jones part of the potential while the full line shows the full potential including the hydrogen bond part.

to allow analytical studies, considers simplified water molecules which have only three arms situated in a plane. This simplification, which would have been a weakness for studies of three dimensional water, is on the contrary a strength for hydration water, because it leads to the correct topology for the network of hydrogen bonds which can be formed between the molecules of hydration water.

In the Ben-Naim model, the interaction potential between two water molecules is the sum of two terms (Fig. 1(b)),

$$U_{ij}(\vec{X}_i, \vec{X}_j) = U_{LJ}(R_{ij}) + U_{HB}(\vec{X}_i, \vec{X}_j) \ , \qquad (3)$$

where $\vec{X}_i$ is a generalized three-component vector which specifies the coordinates x_i, y_i of molecule i in two dimensions and its orientation defined by the angle $\alpha_i = (\vec{i}_1, \vec{x})$ between its first arm and the fixed x axis chosen as a reference, R_{ij} is the distance between molecules i and j, $U_{LJ}(R_{ij})$ is a Lennard-Jones potential between the centers of the molecules, $U_{LJ}(R) = 4\epsilon[(\sigma_0/R)^{12} - (\sigma_0/R)^6]$, parameterized by its energy scale ϵ and range σ_0. The hydrogen-bond potential U_{HB} is split in two factors

$$U_{HB}(\vec{X}_i, \vec{X}_j) = \epsilon_H G_{\sigma'}(R_{ij} - R_H) \sum_{k,l=1}^{3} G_{\sigma}(\vec{i}_k \cdot \vec{u}_{ij} - 1) G_{\sigma}(\vec{j}_l \cdot \vec{u}_{ij} - 1) , \quad (4)$$

where function $G_{\sigma}(x)$ is an unnormalized Gaussian function $G_{\sigma} = \exp(-x^2/\sigma)$. The parameter ϵ_H is negative and sets the energy scale of the hydrogen-bond potential. The first factor indicates that an hydrogen bond has a preferred length R_H, while the second factor, which involves a summation over all pairs of indices k, l that label the three arms of molecules i and j respectively, is an angular term which indicates that hydrogen bonds are preferentially formed when an arm of molecule i is aligned with an arm of molecule j. The vectors $\vec{i}_k$, $\vec{j}_l$ are unit vectors of the arms of the two molecules and $\vec{u}_{ij} = \vec{R}_{ij}/R_{ij}$ is a unit vector along the direction that joins the center of the molecules. The angular term is chosen such that the strongest hydrogen bond is formed when two arms of the water molecules are perfectly collinear, and no distinction is made between donors and acceptors. It is this term which imposes the geometry of the network of hydrogen bonds. The parameters σ' and σ determine the selectivity of the formation of hydrogen bonds with respect to the distance or orientation of the molecules. We have chosen the parameters of the Ben-Naim model in order to get the best agreement with the SCP/E potential which has been extensively tested. They are $\epsilon = 0.016$ eV, $\sigma_0 = 2.625$ Å, $\epsilon_H = -0.192$ eV, $R_H = 2.5$ Å, $\sigma' = 1.5715$ Å^2, $\sigma = 1.8359 \ 10^{-4}$.

Besides its geometry which is suitable for two-dimensional water, the Ben-Naim model has another great advantage over the SCP/E model: it does not require the calculation of Ewald sums which appear when electrostatic interactions are explicitely considered because it replaces the electrostatic interactions by appropriately chosen effective potentials. This model, which is fairly old, has been recently revived in studies of the hydrophobic effect [13].

For free water molecules in two dimensions, the Ben-Naim model captures some experimentally observed properties of real water such as its density anomaly [12][13] and it freezes into an hexagonal ice-like structure at low temperatures. In order to describe the properties of the

hydration water of a protein, we must add an important component, the binding of the molecules to the protein surface which restricts their translational freedom. In our model the protein surface is described by an underlying lattice which corresponds to the favorable sites for hydrogen bond binding.
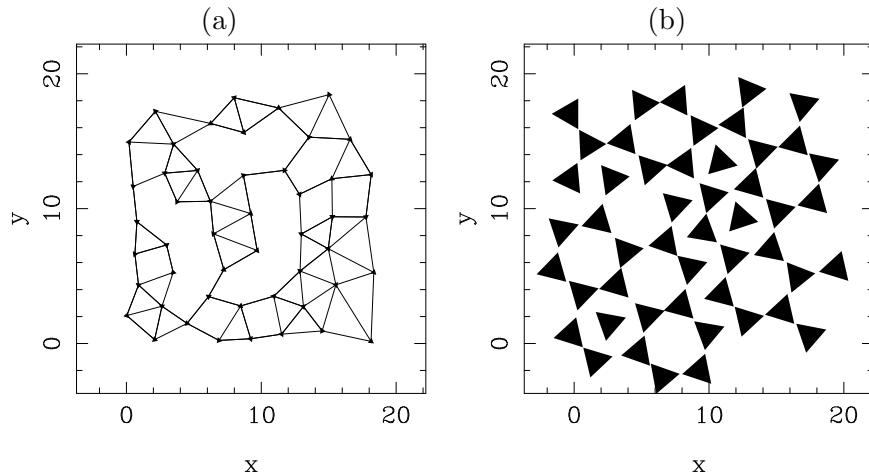
Figure 2. (a) Example of underlying lattice of binding sites for a cluster of 49 water molecules. (b) Structure of the water cluster obtained on this lattice at $T = 0.020$ eV. The water molecules are represented by triangles which show the three directions in which they can form hydrogen bonds.

We do not attempt to describe the actual geometry of the protein surface. Instead we are using a disordered network of binding sites. However this network must not be fully random. Two water molecules cannot bound to two sites which are too close to each other, and, since we are interested in percolated water clusters, the binding sites must not be too far from each other either. In order to generate an underlying disordered lattice that meets these criteria, we start from a set of points randomly chosen inside a selected spatial region which determines the size of the cluster. We assume that these points are connected by the same Lennard-Jones potentials which binds the molecule centers in the Ben-Naim model. Then we perform an incomplete Monte-Carlo (MC) relaxation of the energy of this lattice which moves the sites in order to relax the major constraints introduced by points which are too close to each other. The number of MC steps determines the amount of residual disorder. A typical underlying lattice for a water cluster of 49 molecules is shown on Fig. 2. Once the underling lattice has been chosen, one water molecule is attached to each site by an

harmonic potential $U_{loc} = \epsilon_{loc}r^2$, where r is the distance between the water molecule and its binding site in the underlying lattice.

$$T = 0.040eV$$

$$T = 0.020eV$$
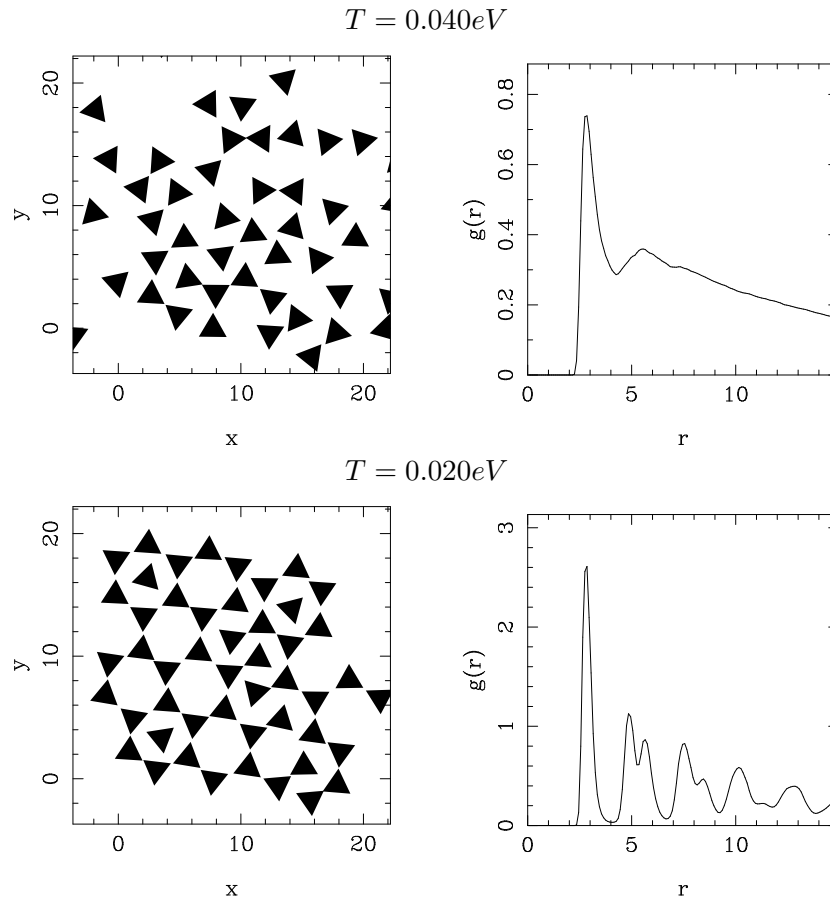
Figure 3. Examples of the structure of the two-dimensional water model and the corresponding radial distribution function $g(r)$ at two temperatures (measured in energy units.

The value of ϵ_{loc} depends on the substrate but it is is not critical although it modifies quantitatively the results. We show here two cases that differ by one order of magnitude: $\epsilon_{loc} = 0.244 \ 10^{-2}$ eV/Å^2 which is such that the frequency of the small amplitude vibrations of a water molecule in its translation parallel to the surface, that can be performed by bond rotations, is one seventh of the frequency associated to the stretching of a hydrogen bond, and a larger value $\epsilon_{loc} = 0.244 \ 10^{-1}$ eV/Å^2 corresponding to strongly bound water. The important feature is the presence of the underlying lattice which has a structure and a connectivity which does not correspond to the equilib-

rium ice-like structure that the water molecules would chose if they were freely moving in space. This introduces a *frustration* which strongly influences the structure and dynamics of the water clusters.

The Ben Naim model of water combined with the disordered lattice of attachment sites makes the model of hydration water which is at the basis of the analysis of the dielectric measurements in our approach. For this purpose we investigate the thermodynamics and dynamics of this model system with Monte Carlo simulations.

3.2. STRUCTURAL PROPERTIES.

Starting from an arbitrary configuration of the water molecules, the relaxation of the the water cluster toward its equilibrium configuration determines its structure as a function of temperature.
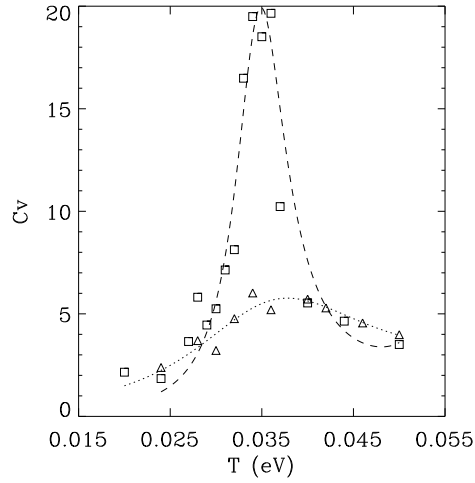
Figure 4. Specific heat per particle versus T (in energy scale) for a cluster of $N = 49$ water molecules. The points are the MC results: squares $\epsilon_{loc} = 0.244 \ 10^{-2}$ eV/Å^2, triangles $\epsilon_{loc} = 0.244 \ 10^{-1}$ eV/Å^2. The dash and dotted lines are guides to the eye obtained by fitting the numerical points with the expression $C_v = A/(1 + B(T - T_0)^2 + C(T - T_0)^3$, where A, B, C, and T_0 are parameters.

Structural data on the water cluster are provided by the static pair correlation function $g(r)$ (Fig. 3). As one might expect, at high temperatures, the water molecules have large amplitude fluctuations around their binding positions and $g(r)$ is similar to the pair distribution function of liquid water. It shows a peak around $r = R_H$ and

is almost featureless for large r. On the contrary, at low temperature, $g(r)$ shows a series of peaks indicating a rather organized structure, which is however not as regular as in a solid because the binding of the water molecules to the protein surface prevents a crystallization into a regular ice structure. The high an low temperature domains are separated by a smooth transition which can be detected by a broad maximum of the specific heat per particle (Fig. 4), deduced from the fluctuations of the energy E of the cluster of N molecules in the MC iterations $C_v = (\langle E^2 \rangle - \langle E \rangle^2)/[N(k_B T)^2]$. The width of the transition region depends on the strength of the interaction with the underlying disordered lattice. Increasing ϵ_{loc} broadens the transition.

3.3. DYNAMICS OF THE HYDRATION WATER.

In order to make the link with the dielectric measurements, it is necessary to characterize the fluctuations of the network of hydrogen bonds. This can be done by monitoring the *cage correlation function* [14] $C(t)$ which measures the rate of change of the hydrogen bond network around each molecule. It can be defined as follows: at time t_0, determine for each molecule i the neighboring molecules and the indices of the arms of these molecules which are hydrogen bonded to the arms of molecule i. This defines the "cage" of molecule i. At a later time t, if nothing has changed in the cage of molecule i, set $C_i = 1$, and, if anything has changed (index of a neighbor, broken hydrogen bond, or index of the linked arms), set $C_i = 0$. The cage correlation function is then defined by the sum of the C_i's over the cluster, $C(t) = \sum C_i$. As time evolves, $C(t)$ decreases, but it does not drop to zero because the molecules are attached to the underlying lattice. The neighbors of each molecule are fixed so that the hydrogen bonds that it can make belong to a finite set.

The time evolution of $C(t)$ measures the persistence of a configuration of the network of hydrogen bonds. At high temperature ($T \geq 0.035$ eV), we observe a very fast decay of the cage correlation, which is not surprising since $g(r)$ shows that the system is in a liquid state. The intermediate temperature range (0.025 eV$< T < 0.035$ eV) is the most interesting because the $C(t)$ shows a slow, non exponential decay, which is well described by a *stretched exponential* behavior

$$C(t) = C_0 \exp\left[-\left(\frac{t}{\tau}\right)^\beta\right] + C_1 \qquad 0.3 \leq \beta \leq 0.6 , \qquad (5)$$

as shown in Fig. 5.a. When T is decreased below 0.025 eV, $\beta \to 1$, i.e. $C(t)$ recovers a simple exponential decay, with a very long correlation time τ, indicating that the water cluster is almost frozen.

(a)   (b)
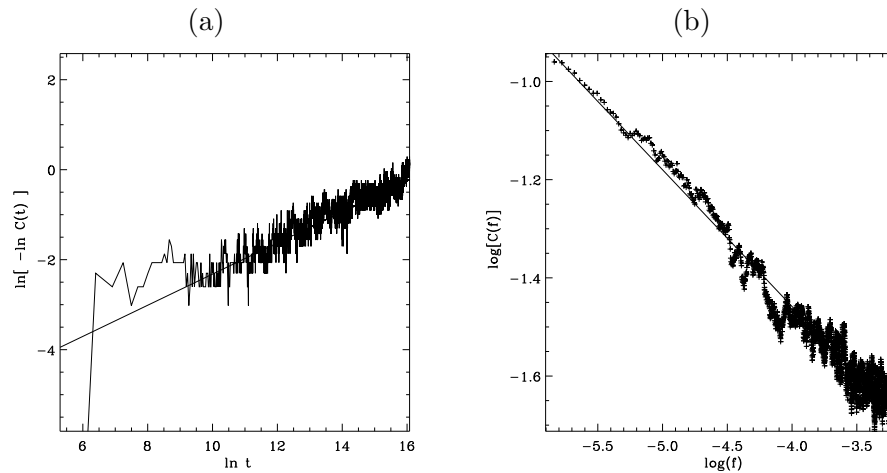
Figure 5. (a) Time evolution of the cage correlation function $C(t)$. The figure shows $\ln[\ln(C(t)]$ versus $\ln(t)$. (b) Spectrum of the fluctuations of the cage correlation function $C(f)$, in logarithmic scale.

When $C(t)$ has decayed to its average value, the spectrum of its fluctuations provides another measurement of the dynamics of the formation and breaking of the hydrogen bonds (Fig. 5.b). It shows a power law $C(f) \propto 1/f^{\alpha}$ over about three decades, with $\alpha = 0.25 \pm 0.05$ in the transition region, indicating the existence of a broad range of time scales, dominated by slow fluctuations.

4. Discussion and conclusion.

The cage correlation function, which reflects the dynamics of the hydrogen bonds in the cluster, appears to be consistent with the dielectric measurements. The stretched exponential relaxation of the cage correlation function, which is typical of a glassy behavior, can explain the experimental observation of a proton glass. A schematic picture of the relaxation frequency versus temperature emerging from our analysis is shown in Fig. 6.

Proton transfers between water molecules can involve two mechanisms. As discussed is Sect. 2, they can be assisted by the dynamics of the water molecules. In this case the dielectric measurements simply reflect of the dynamics of the water. Below the glass transition of the water network, these "assisted proton transfers" become extremely slow because the water network is almost frozen. In this low temperature range, a second mechanism starts to dominate, the thermally
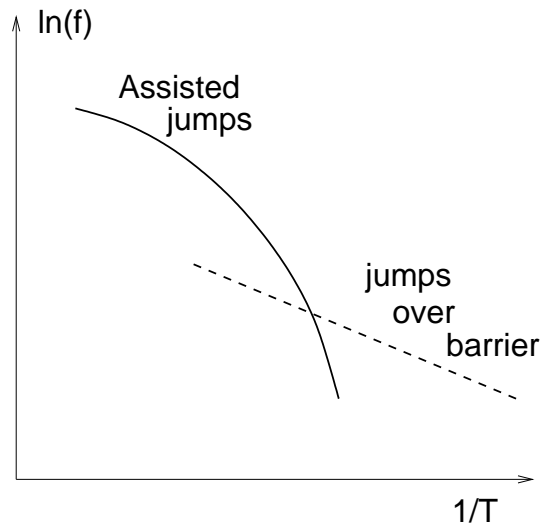
Figure 6. Schematic picture of the evolution of the logarithm of the dielectric relaxation frequency f versus inverse temperature showing the suggested basic mechanisms of this relaxation.

activated proton jumps over the potential barrier which exists when water molecules are at their equilibrium distance. This barrier is high compared to the thermal energies of the protons. Consequently thermal jumps are rare events, hidden by the assisted jumps above the glass transition. They only show up when the assisted jumps are too rare as schematized on Fig. 6. In this low temperature range, as the water network is disordered due to the links to the underlying protein surface, one has to consider the thermal diffusion of protons over a set of random barriers. This problem has been treated by Zwanzig [15]. For a Gaussian distribution of barriers, the diffusion coefficient evolves as $D \propto \exp\left[-E^2/T^2\right]$. Although this behavior does not agree with the statement of an Arrhenius behavior at low temperature made for the dielectric measurements [5, 6], one has to notice that the dielectric measurements are only available in a small temperature range below the glass transition 250 K$< T <$ 270 K. In such a range the evolution given by Zwanzig's calculation is almost indistinguishable from a true Arrhenius behavior.

The picture discussed above is also consistent with the observation of slightly different glass transition temperatures for different relaxation frequencies because Each water patch has its own characteristic frequency determined by its size and the proton mobility that depends on the underlying lattice structure, and moreover each patch has its tran-

sition temperature which is also dependent on the size and underlying lattice.

Therefore we have connected the glass transition observed in the proton dynamics to a glass transition of the water molecules themselves. The freezing of the water dynamics is consistent with the observation of a fast change in water thermal motions below 270 K for weakly hydrated myoglobin [1]. The Ben-Naim potential is only a simplified description of water molecule interactions, however it provides a good picture for the geometry of the hydrogen bonds. Combined with the frustration that comes from the underlying protein binding sites, it leads to a glassy behavior, showing that long range electrostatic interactions are not crucial. The present study cannot claim to a complete description of "two-dimensional water", but, as the MC studies of water clusters and dielectric measurements point toward the same direction, it suggests that the hydration water of proteins, and perhaps also of porous materials, could provide an interesting system to study some of the properties of supercooled or glassy water, and that dielectric measurements are a useful tool for such a study. The recent observation [16] of similar smooth transition in the range $240 - 250$ K by neutron scattering on water adsorbed on vycor glass suggests that the ideas included in the present model are sufficiently general to extend beyond the case of protein hydration water. In the protein case the role of the ionization of the side chains to inject protons and the influence of the dynamics of the protein that would lead to a deformable underlying lattice instead of a set of fixed binding sites have to be considered.

Moreover the results of the dielectric measurements which exhibit long range charge transport on the protein surface suggest that, in the studies of protein activity and folding, the role of charge transport should not be neglected. A similar observation was made by Singh et al. [17] who compared the microwave dielectric relaxation rate and the conformational fluctuation rate measured by Mössbauer effect. For theoretical studies of protein folding these observations lead to the conclusion that position dependent interaction potential should be considered is the model does not explicitly include water and charge transport because folding must imply some charge motions on the protein surface induced by the electric interactions, which, in turn, means that the forces between the various parts of the protein change as the folding goes on.

References

1. Sartor G., Hallbrucker A., Hofer K. and Mayer E., Calorimetric glass-liquid transition and crystallization behavior of a vitreous, but freezable, water fraction of hydrated methemoglobin. *J. Phys. Chem.* **96** (1992), 5133-5138

2. Rupley J. and Careri G.: Protein hydration and function, *Advances in Protein Chemistry* **41** (1991), 37-172

3. Reinisch L., Kaiser R.D. and Krim J.: Measurement of protein hydration shells using a quartz microbalance, *Phys. Rev. Lett.* **63** (1989), 1743-1746

4. Careri G., Geraci M., Giansanti A. and Rupley J.A., Protonic conductivity of hydrated lysozyme powders at megahertz frequencies. *Proc. Natl. Acad. Sci. USA* **82** (1985), 5342-5346

5. G. Careri, G. Consolini and F. Bruni, Dielectric relaxation of a proton glass in hydrated protein powders. *Solid State Ionics* **125** (1999), 257-261

6. A. Levstik, C. Filipic, Z. Kutnjak, G. Careri, G. Consolini and F. Bruni, Proton glass freezing in hydrated lysozyme powders. *Phys. Rev. E* **60** (1999), 7604-7607 (1999)

7. E. Courtens, Scaling dielectric data on $Rb_{1-x}(NH_4)_x H_2 PO_4$ structural glasses and their deuterated isomorphs. *Phys. Rev. B* **33** (1986), 2975-2978

8. M. Kunst and J.M. Warman, Proton mobility in ice. *Nature* **228** (1980), 465

9. J. Lobaugh and G. A. Voth, The quantum dynamics of an excess proton in water. *J. Chem. Phys.* **104** (1996), 2056-2069

10. F.W. Starr, J.K. Nielsen and H.E. Stanley, Fast and slow dynamics of hydrogen bonds in liquid water, *Phys. Rev. Lett.* **82**, (1999) 2294-2297

11. A. Ben-Naim, Statistical mechanics of "waterlike" particles in two dimensions. I. Physical model and application of the Percus-Yevick equation. *J. Chem. Phys.* **54** (1971), 3682-3695

12. A. Ben-Naim, Statistical mechanics of "waterlike" particles in two dimensions. II. One component system. *Molecular physics* **24** (1972), 705-721

13. K.A.T. Silverstein, A.D.J. Haymet and K.A. Dill, A simple model of water and the hydrophobic effect, *J. Am. Chem. Soc.* **120** (1998), 3166-3175

14. E. Rabani, D. Gezelter and B.J. Berne, Direct observation of stretched exponential relaxation in low-temperature Lennard-Jones systems using the cage correlation function. *Phys. Rev. Lett.* **82** (1999), 3649-3652

15. R. Zwanzig, Diffusion in a rough potential. *Proc. Natl. Acad. Sci. USA* **85** (1998), 2029-2030

16. J.-M. Zanotti, private communication.

17. G.P. Singh, F. Parak, S. Hunklinger and K. Dransfeld, Role of adsorbed water in the dynamics of metmyoglobin. *Phys. Rev. Lett.* **47** (1981) 685-688.